

Rateless Autoencoder Codes: Trading off Decoding Delay and Reliability

Vukan Ninkovic,* Dejan Vukobratovic,* Christian Häger,† Henk Wymeersch,† and Alexandre Graell i Amat†
*University of Novi Sad, Novi Sad, Serbia

†Department of Electrical Engineering, Chalmers University of Technology, Gothenburg, Sweden

Abstract—Most of today’s communication systems are designed to target reliable message recovery after receiving the entire encoded message (codeword). However, in many practical scenarios, the transmission process may be interrupted before receiving the complete codeword. This paper proposes a novel rateless autoencoder (AE)-based code design suitable for decoding the transmitted message before the noisy codeword is fully received. Using particular dropout strategies applied during the training process, rateless AE codes allow to trade off between decoding delay and reliability, providing a graceful improvement of the latter with each additionally received codeword symbol. The proposed rateless AEs significantly outperform the conventional AE designs for scenarios where it is desirable to trade off reliability for lower decoding delay.

I. INTRODUCTION

The design of short block-length error-correcting codes for unpredictable and time-varying wireless channels still remains a challenge [1]. Particularly challenging is the design of codes for channels experiencing prolonged deep fades or even complete channel failures that prevent the receiver to receive the complete (noisy) codeword. Such channels, referred to as *dying channels* in [3] and [4], arise in various communication systems, e.g., due to loss of synchronization, lack of memory, depletion of harvested energy in wireless sensors, interruption of a secondary user by a primary user in cognitive radio, loss of line-of-sight channel in optical wireless communications, limited channel duration of low-earth-orbit satellite communications, or physical defects in magnetic recording memories [4]–[6]. Despite their apparent applicability, few works have considered the design of coding schemes for dying channels [5]–[7].

In the above-mentioned scenarios, a conventional fixed-rate code design may suffer from high inefficiency in the short block-length regime. Rateless codes provide a possibility for the receiver to trade off decoding delay with increased reliability by adaptively receiving additional codeword symbols (thus decreasing the code rate) until the desired reliability is attained [8]. Rateless codes such as rateless spinal codes [9] and analog fountain codes (AFC) [10] are recent classes of codes that represent a flexible solution for rate adaptation to unpredictable wireless channels. Both spinal and AFC codes map the set of input messages directly into codewords comprising sequences of real (or complex) symbols, thus effectively performing adaptive coding and modulation.

This paper has received funding from the European Union’s Horizon 2020 research and innovation programme under Grant Agreement number 856967.

Deep autoencoders (AEs) provide a new framework to design codes for challenging—or unknown—channels [11]. AE-based codes have been studied in several settings, such as one-bit quantization channels [12], optical communications [13], and OFDM [14]. The resulting AE-based codes are shown to perform close to optimal for several baseline scenarios [11]–[15]. Similar to spinal and AFC codes, AE-based codes map input messages directly into real (or complex) codeword sequences. However, AE-based codes are trained—and thus optimized—for a given code rate, meaning that they perform poorly if the decoding is attempted before the complete codeword is received.

Designing flexible and efficient short block-length codes for dying channels [4] is the focus of this paper. In particular, we extend the conventional AE-based code design to a class of AE-based codes that shares with rateless codes that receiving additional codeword symbols progressively improves the successful message decoding probability. We call the proposed AE-based codes *rateless AE codes*. Such progressive improvement of the reliability allows the receiver to select when, i.e., after how many received symbols, to attempt decoding, thus trading off error probability with decoding delay. Inspired by a recent work on rateless AEs for flexible reduced-dimensionality signal representation [16], we integrate suitably designed dropout strategies into the AE-based code design to induce the desired performance behavior. More precisely, by controlling the dropout parameters in rateless AE code design, we shape a desired decoding delay vs reliability behavior of the resulting codes: a property that is not easy to enforce using classical coding approaches. Numerical results demonstrate that the resulting rateless AE codes significantly outperform conventional AE-based code designs for scenarios where it is desirable to trade off reliability for lower decoding delay such as the case of dying channels.

II. SYSTEM MODEL AND AUTOENCODER-BASED CODES

A. System Model

We consider a transmitter that sends a message m from a message set $\mathcal{M} = \{1, 2, \dots, M\}$ over a noisy channel. Each message is represented as a sequence of $k = \log_2(M)$ bits $\mathbf{s} = (s_1, s_2, \dots, s_k)$. The encoder encodes a message m into a transmitted codeword $\mathbf{x} = (x_1, x_2, \dots, x_n)$ of length n symbols. Formally, we define the encoder via the function $f : \mathcal{M} \rightarrow \mathbb{R}^n$. We consider two different power constraints for the codewords: i) a fixed power constraint, for which

$\|\mathbf{x}\|_2^2 = n$ holds for every \mathbf{x} , and ii) and average power constraint, for which $\frac{1}{M} \sum_{i=1}^M \|\mathbf{x}_i\|_2^2 = n$. The code rate is defined as $R = k/n$ [bits/channel use].

Let $\mathbf{y} = (y_1, y_2, \dots, y_n) \in \mathbb{R}^n$ be the output of the channel (described in the next subsection). The decoder maps \mathbf{y} into the estimated message \hat{m} using the decoder transform $g: \mathbb{R}^n \rightarrow \mathcal{M}$.

B. Channel Model

We consider a channel model consisting of the cascade of an AWGN channel and an erasure channel. The motivation underpinning this model is to consider an AWGN channel affected by random interruptions or occasional *deep fades*—modeled as erasures—whose locations are known to the receiver (see Section II-C below for more details). Let E_b/N_0 denote the energy per bit (E_b) to noise power spectral density (N_0) ratio.

We consider two variants of the proposed cascaded AWGN and erasure channel, as detailed below. In both models, the erasure channel is described by a set of L channel states. We denote by p_ℓ the probability that the channel is in the ℓ -th state. The erasure channel state distribution is defined as $\mathbf{p} = \{p_1, p_2, \dots, p_L\}$, $\sum_{\ell=1}^L p_\ell = 1$.

Model 1: Channel Model with Tail Erasures. In this model, the receiver receives the first r_ℓ symbols of \mathbf{y} and the remaining $n - r_\ell$ symbols are erased. The ℓ -th channel state is then defined by the pair (p_ℓ, r_ℓ) ; if the erasure channel is at state ℓ , the receiver receives $\mathbf{y}_\ell = \{y_1, y_2, \dots, y_{r_\ell}\}$, while the remaining symbols are erased. Let $\mathbf{r} = \{r_1, r_2, \dots, r_L\}$. The channel model with tail erasures is then defined by \mathbf{p} and \mathbf{r} .

Model 2: Channel Model with Random Erasures. In this model, the symbols of \mathbf{y} are randomly erased. The ℓ -th state of the erasure channel is defined by a pair (p_ℓ, ϵ_ℓ) , where $\epsilon_\ell \in [0, 1]$ is the symbol erasure probability. The L channel states are defined by \mathbf{p} and the set of corresponding erasure probabilities $\boldsymbol{\epsilon} = \{\epsilon_1, \epsilon_2, \dots, \epsilon_L\}$.

C. Comment on the Channel Models

Model 1 is known as a *channel that dies*, and its information-theoretic properties are investigated in [4]. The model is suitable for situations where the receiver, after receiving a certain (varying) number of symbols, can no longer receive additional symbols. This may be the case with low-cost devices due to, e.g., loss of synchronization, lack of memory, or depletion of harvested energy, in satellite communications, molecular communications, and in certain magnetic recording cases. The model is also motivated by a scenario where a receiver is able to trade off decoding delay against error probability by performing decoding based only on the first received symbols: The error probability decreases with each received symbol at the expense of an increased delay. Depending on the error rate and delay requirements, the receiver can decide when to start the decoding process.

Model 2 is a multi-state extension of a channel model, dubbed AWGN+erasure channel, considered in [17]. This model, as well as the model with tail erasures, is also suitable to model multicast to heterogeneous receivers. In this case,

the erasure channel state probabilities model the fraction of receivers experiencing different erasure channel states. In our context, the model with random erasures is used as a reference for comparison with the tail erasure channel model.

D. Problem Formulation

Under the setup in Section II-B, the goal is to design a pair (f, g) that, for a given number of received symbols, minimizes the average message error probability

$$P_e = \frac{1}{M} \sum_{m \in \mathcal{M}} \mathbb{P}\{\hat{m} \neq m | m\}. \quad (1)$$

Before presenting the proposed rateless AE code design, we review the basics of the conventional AE-based codes.

III. PRELIMINARIES: CONVENTIONAL AUTOENCODER-BASED CODE DESIGN

From the deep learning perspective, the communication system described in Section II-A can be implemented as an autoencoder (AE) [11], as illustrated in Fig. 1 (disregard for the moment the dropout block). The input (encoder) and output (decoder) layers and the bottleneck layer constitute the main AE blocks. The AE-based approach introduces a new design paradigm in communication systems in which the transmitter and receiver components are jointly optimized using machine learning-based end-to-end learning methods.

At the transmitter's input layer, the message m is encoded as a one-hot vector $\mathbf{u} = (u_1, u_2, \dots, u_M) \in \{0, 1\}^M$, i.e., it is represented as an M -dimensional vector with the m -th element equal to one and all other elements equal to zero. The transmitter can be represented as a feedforward neural network with H hidden layers, followed by a bottleneck layer of width n (corresponding to the codeword length). At the output of the bottleneck layer, a normalization step ensures that the power constraint on \mathbf{x} is met. The number of neurons in each hidden layer is given by the vector $\mathbf{h} = \{h_1, h_2, \dots, h_H\}$, where h_i represents the number of neurons of the i -th hidden layer.

The AWGN channel is implemented by the noise layer. The output of the noise layer can be represented as $\mathbf{y} = \mathbf{x} + \mathbf{z}$, where \mathbf{z} contains n independent and identically distributed samples of a Gaussian random variable with zero mean and variance σ^2 . It is important to notice that the random nature of the channel can be represented as a form of regularization, because the receiver never sees the same training example twice. As a consequence, it is almost impossible for the neural network to overfit [15].

The goal of the neural network is to find the most suitable representation of the information robust to the channel perturbations. The receiver is implemented in the same way as the transmitter (symmetric feedforward neural network), except that the last layer has a softmax activation function with output $\mathbf{b} = (b_1, b_2, \dots, b_M) \in (0, 1)^M$, $\|\mathbf{b}\|_1 = 1$. The index of the highest value element in \mathbf{b} corresponds to the decoded message \hat{m} , i.e.,

$$\hat{m} = \arg \max_i \{b_i\}.$$

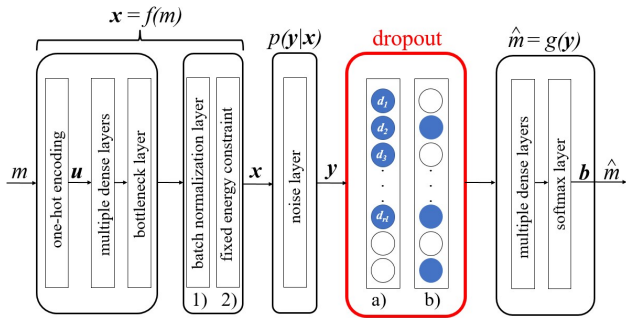


Fig. 1. Communication system represented as a deep autoencoder [11] with two types of normalization: 1) Average power constraint and 2) Fixed power constraint; and dropout block for: a) Model 1 and b) Model 2.

Except for the last layer of the transmitter and receiver, which have linear and softmax activation functions respectively, all others layers use the rectified linear unit (ReLU) as the activation function.

Ideally, one would like to train the AE to minimize the error probability P_e . However, P_e cannot be used directly as it is not differentiable. A common approach is to use the cross-entropy loss between \mathbf{u} and \mathbf{b} ,

$$\ell(\mathbf{u}, \mathbf{b}) = - \sum_{i=1}^M u_i \log b_i, \quad (2)$$

as a surrogate for the error probability. The AE is then trained so that $\ell(\mathbf{u}, \mathbf{b})$ is minimized.

IV. RATELESS AUTOENCODER CODES

A. Design of Rateless Autoencoder Codes

We introduce a novel class of AE codes, referred to as rateless AE codes, that allow to trade off decoding delay and reliability. Inspired by the rateless AEs in [16], we use a suitably defined *randomized dropout* strategy to match the AE-based code design to a given erasure channel model. To define a generic randomized dropout strategy covering various erasure channel models, we introduce a channel dropout vector \mathbf{d} associated to the channel noise layers, as shown in Fig.1. A channel dropout vector $\mathbf{d} = (d_1, d_2, \dots, d_n)$, $d_i \in \{0, 1\}$, is a binary vector of length n whose zero entries (represented by empty circles in the dropout block in Fig. 1) designate noise layer neurons on which the dropout is applied, i.e., whose output values are set to zero [18]. To address the erasure channel models with multiple states ($L > 1$), we define a sequence of dropout vectors $\mathbf{d}_\ell, \ell \in \{1, 2, \dots, L\}$, where dropout vector \mathbf{d}_ℓ corresponds to the ℓ -th class. The number of zeros and ones and their positions or statistical occurrence in the dropout vectors $\{\mathbf{d}_\ell\}$ are defined as part of the rateless AE code design process.

In the training process, we apply the randomized dropout strategy, where different dropout vectors are applied randomly on a batch-by-batch basis. For each training batch, we first randomly sample a dropout class $\ell \in \{1, 2, \dots, L\}$ following

the dropout class probability distribution \mathbf{q} , and then apply the dropout vector \mathbf{d}_ℓ corresponding to the dropout class ℓ for all the training samples in the batch. The details of applying dropout vectors on individual training batches differ for each of the erasure channel models defined in Section II-B, as we detail next.

Model 1. The dropout vector \mathbf{d}_ℓ for the ℓ -th class is constructed such that its first r_ℓ positions (corresponding to the topmost neurons in the layer) are set to one, while the remaining ones are set to zero (recall that only the first r_ℓ symbols survive the channel unerased), as shown in Fig. 1 (dropout block a)). Note that each dropout vector \mathbf{d}_ℓ is fixed in advance, i.e., it is deterministic.

Model 2: The dropout vector \mathbf{d}_ℓ for the ℓ -th class (characterized by the channel erasure probability ϵ_ℓ , see Section II-B) is constructed so that each of its positions is randomly and independently set to zero with probability ϵ_ℓ , as shown in Fig. 1 (dropout block b), empty circles represent zero neurons). Note that each dropout vector \mathbf{d}_ℓ is now randomized, i.e., the realization of \mathbf{d}_ℓ is random and in general different across the training batches.

B. Connections to Rateless and Rate-Compatible Codes

The proposed AE codes provide a graceful degradation of the error probability as additional codeword symbols are received (see Sec. V). This behavior is akin to rateless codes, justifying the nickname *rateless AE codes*. However, strictly speaking, the proposed codes are not rateless in the sense that an arbitrary number of codeword symbols can be generated from the source message. In the context of latency-constrained communications, one can set the codeword length n to a sufficiently large value, e.g., to the value which corresponds to the maximum allowable decoding delay.

From the receiver perspective, rateless AE codes allow flexible selection of the codeword length. In this sense, the proposed codes are related to rate-compatible codes for incremental redundancy hybrid automatic repeat request (HARQ) [19]. Note also that, for any selected codeword length, we are interested in decoding the complete source message. This is in contrast to optimizing the intermediate performance of rateless codes that targets recovery of a part of the message if an insufficient number of codeword symbols are received [20]. It is also different from unequal error protection codes that provide certain messages or parts of a message a higher probability of reconstruction, as we recently investigated in the context of AE-based code design [21].

V. PERFORMANCE EVALUATION OF RATELESS AE CODES

The goal of this work is to devise a code design that is able to trade off decoding delay against decoding error probability. To the best of our knowledge, code design for fading channels has only been addressed for the binary erasure channel (BEC) [5], [6]. Thus despite their apparent importance, explicit constructions of codes for channel models 1 and 2 above are missing. In this work, we use an AE-based approach to address this problem.

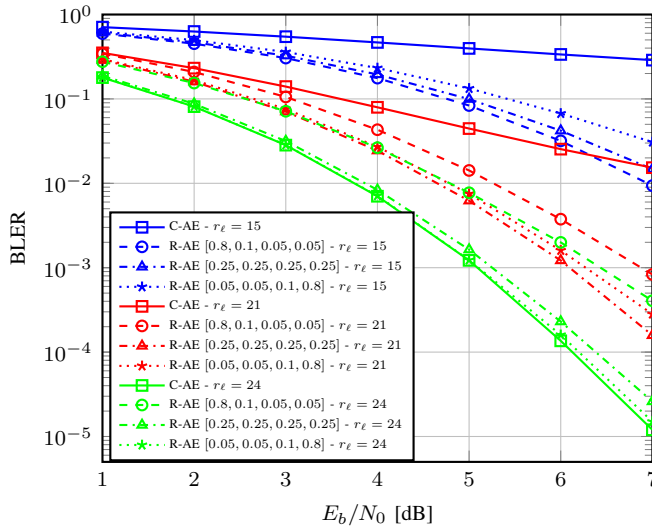


Fig. 2. Rateless AE (R-AE) versus Conventional AE (C-AE) decomposed BLER performances for different erasure channel state distributions \mathbf{p} (Model 1, $(n, k) = (24, 12)$).

We present results for the $(n, k) = (24, 12)$ code scenario, where $M = 4096$ messages are transmitted over $n = 24$ channel uses. We consider a cascaded AWGN and erasure channel as described in Section II-B.

A. Rateless AE Architecture and Training Procedure

The same training process as for the conventional AE [11], apart from the introduction of appropriate dropout strategies, is preserved for the rateless AE training. More precisely, the rateless AE is optimized by using stochastic gradient descent with the Adam optimizer [22]. The learning rate is $\alpha = 0.001$, $\beta_1 = 0.9$ and $\beta_2 = 0.999$. The training is performed at $E_b/N_0 = 1$ dB. For both the conventional and rateless AE design, we apply the average power constraint across the set of codewords in the codebook. This type of normalization can be accomplished by introducing a batch normalization layer in the AE architecture (Fig. 1) [23]. For both the conventional and rateless AE architectures, we consider a single fully-connected hidden layer ($H = 1$) with 500 neurons, i.e., $\mathbf{h} = \mathbf{h}_1 = 500$, and a batch size 500. Both training and test data sets are created by sampling a message set \mathcal{M} uniformly at random. The training and test data set consist of 10^5 and 10^6 messages, respectively.

B. Model 1 – Channel with Tail Erasures

We consider the tail erasure model with $L = 4$ states. In each state, a receiver is able to receive the first $r = \{15, 18, 21, 24\}$ consecutive channel symbols, respectively. The erasure channel state distribution is $\mathbf{p} = \{p_1, p_2, p_3, p_4\}$ (whose numerical values are specified later). Assuming that \mathbf{p} and \mathbf{r} are known at the transmitter, the channel dropout distribution \mathbf{q} and vectors \mathbf{d}_ℓ are constructed to match the tail erasure channel parameters \mathbf{p} and \mathbf{r} . In other words, we set $\mathbf{q} = \mathbf{p}$ and, using \mathbf{r} , we define how many neurons starting from the topmost will survive the dropout for each dropout

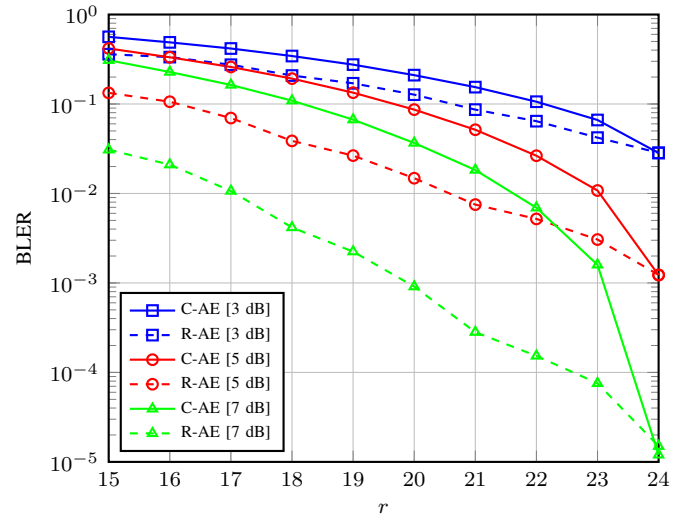


Fig. 3. R-AE versus C-AE BLER performances as a function of the number of received symbols (Model 1, $(n, k) = (24, 12)$).

vector class \mathbf{d}_ℓ . Using the above parameters, we compared the rateless AE design to the conventional AE design.

In Fig. 2, we present block error-rate (BLER) results of rateless AE codes as a function of E_b/N_0 for erasure channel state distributions $\mathbf{p}^{(1)} = \{0.8, 0.1, 0.05, 0.05\}$, $\mathbf{p}^{(2)} = \{0.25, 0.25, 0.25, 0.25\}$ and $\mathbf{p}^{(3)} = \{0.05, 0.05, 0.1, 0.8\}$. For example, for the channel with state distribution $\mathbf{p}^{(1)}$, the probability that first $r_1 = 15$ symbols are received is $p_1 = 0.8$, the first $r_2 = 18$ symbols are received is $p_2 = 0.1$, and so on. The BLER results are presented as follows: for a different number of received symbols $r_1 = 15$, $r_3 = 21$ and $r_4 = 24$ (note that we skip $r_2 = 18$ for the sake of figure clarity), separate BLER curves are presented for each erasure channel state distribution $\mathbf{p}^{(1)}$, $\mathbf{p}^{(2)}$ and $\mathbf{p}^{(3)}$. We compare the BLER results with the conventional AE codes under the same settings. One can note clear performance loss of conventional AE codes as long as they do not receive all n channel output symbols, unlike rateless AE codes whose BLER values degrade more gracefully. From Fig. 2, influence of different dropout class distributions \mathbf{q} (matched to different channel erasure state distribution \mathbf{p}) can be clearly observed. For example, if $\mathbf{q} = \mathbf{p}^{(1)}$ is applied during the training (which favors dropout vector \mathbf{d}_1 with the first $r_1 = 15$ ones), such a code will naturally demonstrate the best BLER performance after receiving the first 15 symbols. In contrast, if trained for the probability distribution $\mathbf{q} = \mathbf{p}^{(3)}$ that favors reception of all n symbols, the rateless AE performance after $r_\ell = n = 24$ symbols is comparable to the conventional AE BLER trained for reception of the complete codeword, while still providing significant BLER improvement for lower r_ℓ values.

Fig. 3 illustrates the BLER performance for the rateless AE design matched to the channel state distribution $\mathbf{p}^{(3)}$ (i.e., $\mathbf{q} = \mathbf{p}^{(3)}$ and $\mathbf{d}_\ell = \mathbf{r}$) as a function of the number of received symbols r for three different E_b/N_0 values (3dB, 5dB and 7dB). Compared to the BLER curves of the conventional AE

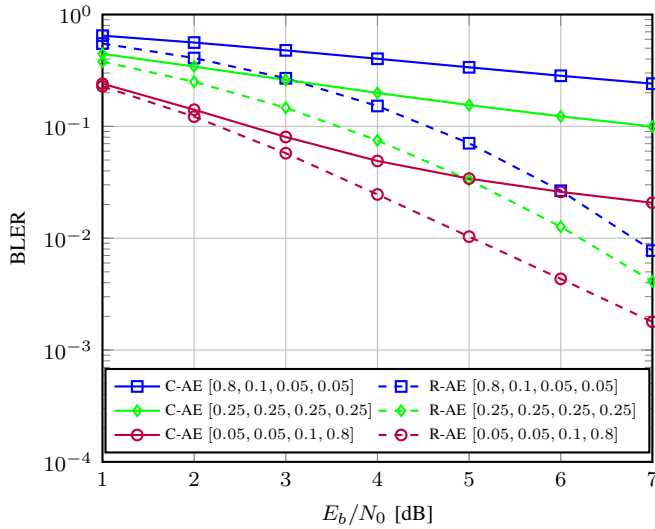


Fig. 4. R-AE versus C-AE averaged BLER performances (Model 1, $(n, k) = (24, 12)$).

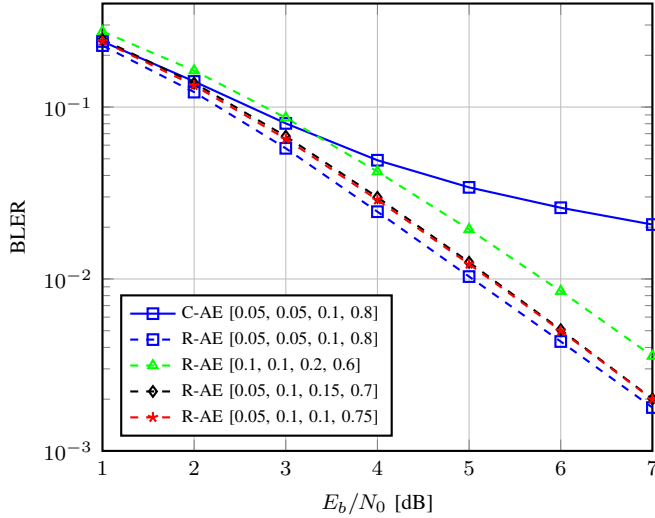


Fig. 5. R-AE (trained for $q = p^{(3)}$) versus mismatched R-AE codes (Model 1, $(n, k) = (24, 12)$).

codes, graceful degradation of BLER curves of the rateless AE codes with the increase of the number of received symbols is clearly observed. Note also that the ability to generalize of the proposed approach is satisfactory, as from Fig. 3, only a slight performance degradation is observed for rates that are not seen during the training process (when r is different than 15, 18, 21 and 24).

In Fig. 4, we present the average BLER curves (averaged across the probability distribution p of the channel erasure states) versus E_b/N_0 (dB) for three different erasure channel state distributions $p^{(1)}$, $p^{(2)}$ and $p^{(3)}$. We note that, by applying an appropriate (i.e., matched) dropout strategy for the rateless AE design, a significant improvement of the average BLER for a given erasure channel state distribution p can be achieved as compared to the conventional AE design.

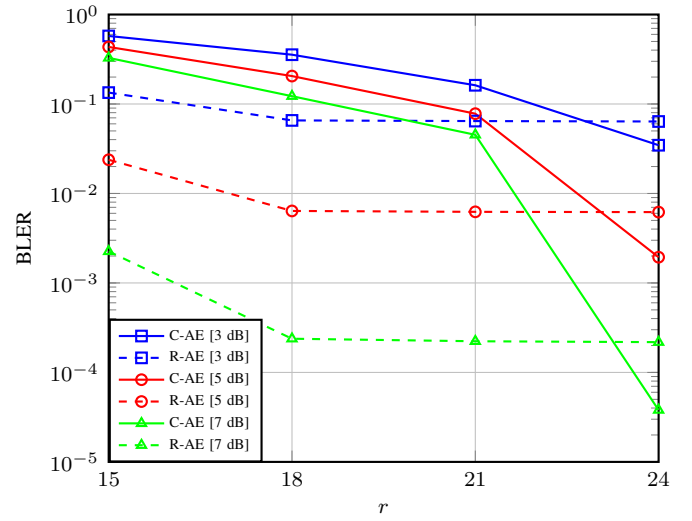


Fig. 6. R-AE versus C-AE BLER performances as a function of the number of received symbols - Fixed power constraint (Model 1, $(n, k) = (24, 12)$).

The previous examples assume that the transmitter knows the erasure channel state distribution p , so that it can apply the matched dropout class distribution $q = p$ for the training process. In order to test the robustness of rateless AE codes on the mismatch of the channel state and the dropout class distributions, in Fig. 5 we examine the average performance of the rateless AE design trained for a particular dropout class distribution $q = p^{(3)}$ against the same code tested over three different mismatched erasure channel state distributions (see the figure legend for details). Clearly, rateless AE design whose dropout class distribution q is matched to the channel state distribution p outperforms the case where the same code is applied over the (slightly) mismatched erasure channel state distribution p . On the other hand, even with mismatch, the proposed rateless AE design significantly outperforms the conventional AE design, demonstrating the inherent robustness of the rateless AE design.

Finally, we emphasize the importance of the power constraint selection. Recall that, herein, we apply the average power constraint, in contrast to the fixed power constraint applied in [11]. In Fig. 6, we present the rateless AE vs the conventional AE BLER performance under the fixed power constraint for the dropout class distribution $q = p^{(2)}$ as a function of the number of received symbols. Besides significant degradation of the conventional AE performance unless all $n = 24$ symbols are received, we note a different behavior of the rateless AE codes that essentially lose their rateless property. In other words, the rateless AE design is now optimized for a specific number of received symbols r which is smaller than the codeword length n (in our example, $r_2 = 18$) and reception of additional symbols does not improve the BLER performance.

C. Model 2 – Channel with Random Erasures

In Fig. 7, we present the average BLER vs E_b/N_0 (dB) results (averaged across different channel erasure states) for

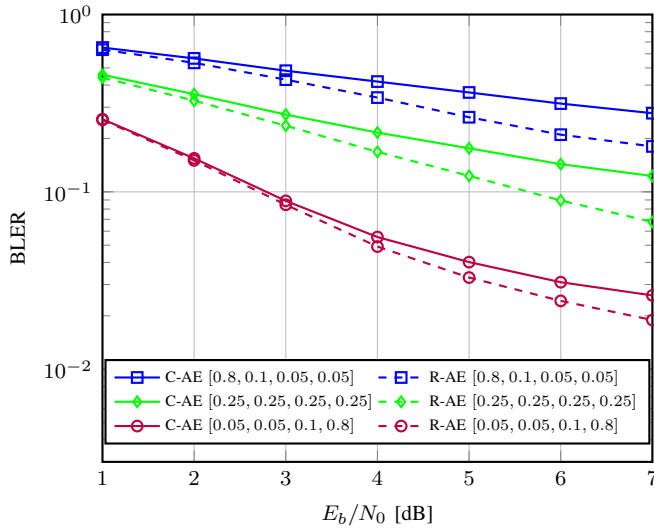


Fig. 7. R-AE versus C-AE averaged BLER performances (Model 2, $(n, k) = (24, 12)$).

$L = 4$ channel erasure states defined by the erasure probabilities $\epsilon = \{3/8, 2/8, 1/8, 0\}$ for three different channel erasure state distributions $\mathbf{p}^{(1)} = \{0.8, 0.1, 0.05, 0.05\}$ (i.e., during the training process, channel erasure probability $\epsilon_1 = 3/8$ will be applied with probability $p_1 = 0.8$, $\epsilon_2 = 2/8$ with probability $p_2 = 0.1$, and so on), $\mathbf{p}^{(2)} = \{0.25, 0.25, 0.25, 0.25\}$ and $\mathbf{p}^{(3)} = \{0.05, 0.05, 0.1, 0.8\}$. As expected, learning the rateless AE code for random erasures is more challenging than for the case of tail erasures, however, the proposed rateless AE design still outperforms the conventional one.

VI. CONCLUSION

We presented rateless AE codes, a novel class of AE codes that trade off decoding delay and reliability. By integrating a randomized dropout technique into the AE-based code design, rateless AE codes provide a graceful degradation of the decoding error probability as a function of the number of received codeword symbols. Rateless AE codes can be tailored for so-called dying channels, where the receiver observes an incomplete noisy codeword interrupted at a given (random) symbol. Such dying channels are relevant in several short-packet wireless communication scenarios. Numerical results demonstrate that the proposed rateless AE codes provide high flexibility in shaping a desired delay vs reliability behavior.

REFERENCES

[1] M. Shirvanimoghaddam, M. S. Mohammadi, R. Abbas, A. Minja, C. Yue, B. Matuz, G. Han, Z. Lin, W. Liu, Y. Li, S. Johnson, and B. Vucetic, "Short block-length codes for ultra-reliable low latency communications," *IEEE Commun. Mag.*, vol. 57, no. 2, pp. 130-137, Feb. 2018.

[2] Y. Polyanskiy, H. V. Poor, and S. Verdú, "Channel coding rate in the finite blocklength regime," *IEEE Trans. Inf. Theory*, vol. 56, no. 5, pp. 2307-2359, May 2010.

[3] M. Zeng, R. Zhang, and S. Cui, "On the Outage Capacity of a Dying Channel," in *Proc. 2008 IEEE Global Commun. Conf. (GLOBECOM)*, New Orleans, LA, USA, Nov. 30- Dec. 4, 2008, pp. 1-5.

[4] L.R. Varshney, S.K. Mitter, and V.K. Goyal, "An information-theoretic characterization of channels that die," *IEEE Trans. Inf. Theory*, vol. 58, no.9, pp. 5711-5724, Sept. 2012.

[5] S. Gu, J. Jiao, Q. Zhang, and X. Gu, "Rateless coding transmission over multi-state dying erasure channel for SATCOM," *Eurasip J. on Wireless Commun. and Netw.*, vol. 2017, no. 1, pp. 1-12, Oct. 2017.

[6] M. Zeng, R. Calderbank, and S. Cui, "On design of rateless codes over dying binary erasure channel," *IEEE Trans. Commun.*, vol. 60, no. 4, pp. 889-894, Apr. 2012.

[7] M. Zeng, R. Zhang, and S. Cui, "Outage Capacity and Optimal Transmission for Dying Channels," *IEEE Trans. on Commun.*, vol. 61, no. 1, pp. 357-367, Jan. 2013.

[8] M. Luby, "LT codes," in *Proc. The 43rd Annu. IEEE Symp. on Found. of Comput. Sci 2002*, Vancouver, Canada, Nov. 16-19, 2002, pp. 271-280.

[9] J. Perry, H. Balakrishnan, and D. Shah, "Rateless spinal codes," in *Proc. 10th ACM Workshop on Hot Topics in Netw.*, Cambridge, MA, USA, Nov. 14-15, 2011, pp. 1-6.

[10] W. J. Lim, R. Abbas, Y. Li, B. Vucetic, and M. Shirvanimoghaddam, "Analysis and Design of Analog Fountain Codes for Short Packet Communications," *IEEE Trans. on Veh. Technol.*, vol. 70, no. 12, pp. 12662-12674, Dec. 2021.

[11] T. O'Shea and J. Hoydis, "An introduction to deep learning for the physical layer," *IEEE Trans. Cogn. Commun. Netw.*, vol. 3, no. 4, pp. 563-575, Dec. 2017.

[12] E. Balevi and J. G. Andrews, "Autoencoder-Based Error Correction Coding for One-Bit Quantization," *IEEE Trans. Commun.*, vol. 68, no. 6, pp. 3440-3451, June 2020.

[13] S. Li, C. Häger, N. Garcia and H. Wymeersch, "Achievable Information Rates for Nonlinear Fiber Communication via End-to-end Autoencoder Learning," in *Proc. 2018 Eur. Conf. on Opt. Commun. (ECOC)*, Roma, Italy, Sept. 23-27, 2018, pp. 1-3.

[14] A. Felix, S. Cammerer, S. Dörner, J. Hoydis and S. Ten Brink, "OFDM-Autoencoder for End-to-End Learning of Communications Systems," in *Proc. IEEE 19th Int. Workshop on Signal Process. Adv. in Wireless Commun. (SPAWC)*, Kalamata, Greece, June 25-28, 2018, pp. 1-5.

[15] S. Dörner, S. Cammerer, J. Hoydis, and S. ten Brink, "Deep learning based communication over the air," *IEEE J. Sel. Topics Signal Process.*, vol. 12, no. 1, pp. 132-143, Feb. 2018.

[16] T. Koike-Akino, and Y. Wang, "Stochastic bottleneck: Rateless autoencoder for flexible dimensionality reduction," in *Proc. IEEE Int Symp. on Inf. Theory (ISIT)*, Los Angeles, CA, USA, June 21-26, 2020, pp. 2735-2740.

[17] A. Sahai, and Q. Xu, "The anytime reliability of the AWGN+erasure channel with feedback," in *Proc. 42nd Allerton Conf. on Commun., Control, and Comput.*, Monticello, IL, USA, Sept. 29- Oct. 1, 2004., pp. 300-309.

[18] N. Srivastava, G. Hinton, A. Krizhevsky, I. Sutskever, and R. Salakhutdinov, "Dropout: A simple way to prevent neural networks from overfitting," *The J. of Mach. Learn. Res.*, vol. 15, no. 1, pp. 1929-1958, June 2014.

[19] D. Declercq, M. Fossorier, and E. Biglieri, *Channel Coding: Theory, Algorithms, and Applications*, Mobile and Wireless Communications Series, Academic Press, 2014.

[20] S. Sanghavi, "Intermediate performance of rateless codes," in *Proc. IEEE Inf. Theory Workshop 2007*, Lake Tahoe, USA, Sept. 2-7, 2007, pp. 478-482.

[21] V. Ninkovic, D. Vukobratovic, C. Haeger, H. Wymeersch, and A. Graell i Amat, "Autoencoder-Based Unequal Error Protection Codes," *IEEE Commun. Lett.*, vol. 25, no. 11, pp.3575-3579, Nov. 2021.

[22] D. P. Kingma and J. L. Ba, "Adam: A method for stochastic optimization," in *Proc. Int. Conf. on Learn. Representation*, San Diego, CA, USA, May 7-9, 2015, pp. 1-41.

[23] N. A. Letizia and A. M. Tonello, "Capacity-Driven Autoencoders for Communications," *IEEE Open J. of the Commun. Soc.*, vol. 2, pp. 1366-1378, 2021.